

Minimally invasive preimplantation genetic testing using blastocyst culture medium

Jiao Jiao¹, Bei Shi², Matthew Sagnelli³, Dalei Yang¹, Yaxin Yao⁴, Wenlu Li⁴, Lin Shao⁴, Sijia Lu^{4,*}, Da Li^{1,*}, and Xiuxia Wang^{1,*}

¹Center of Reproductive Medicine, Shengjing Hospital of China Medical University, 39 Huaxiang Road, Shenyang 110004, China

²Department of Physiology, College of Life Science, 77 Puhe Road, China Medical University, Shenyang 110122, China ³University of Connecticut School of Medicine, 263 Farmington Avenue, Farmington, CT 06030, USA ⁴Department of Clinical Research, Yikon Genomics Company, Ltd., 218 Xinghu Street Suzhou, 215000, China

*Correspondence address. Center of Reproductive Medicine, Shengjing Hospital of China Medical University, Shenyang 110004, China. Tel: +86-18940252099; E-mail: leeda@ymail.com, Tel: +86-18940251898; E-mail: wangxjsj@sina.cn or Department of Clinical Research, Yikon Genomics Company, Ltd., Suzhou, 215000, China. Tel: +86-18911097399; E-mail: lusijia@yikongenomics.com

Submitted on January 16, 2019; resubmitted on April 9, 2019; editorial decision on April 25, 2019

STUDY QUESTION: Is minimally invasive chromosome screening (MICS) using blastocyst culture medium (BCM) sufficiently fast and accurate for preimplantation genetic testing (PGT)

SUMMARY ANSWER: A new assay for MICS, named MICS-Inst achieved high-resolution, comprehensive chromosome ploidy detection using BCM.

WHAT IS KNOWN ALREADY: BCM is a viable source of genomic DNA for use in PGT.

STUDY DESIGN, SIZE, DURATION: Forty-one vitrified blastocysts donated by 22 couples known to carry a chromosome rearrangement and 21 vitrified blastocysts donated from 8 couples with normal karyotypes were used in this study. Good-quality blastocysts, defined as Day 5 and Day 6 embryos \geq BB (AA, AB, BA, BB) based on the Gardner system were used for analysis. Recruitment took place from May 2018 to August 2018. We performed PGT for structural rearrangements (PGT-SR) on 41 BCM, trophectoderm (TE) biopsy and blastocyst-stage embryo (BE) samples as well as PGT for aneuploidies (PGT-A) on 21 BCM, TE biopsy and BE samples.

PARTICIPANTS/MATERIALS, SETTING, METHODS: We made several significant modifications to the BCM composition (mixing blastocoel fluid and spent blastocyst medium) as well as the pre-existing multiple annealing and looping-based amplification cycles (MALBAC) techniques and library generation procedures. The design of a quasilinear preamplification (Pre-AMP) primer and AMP primers 1 and 2 enables the preparation of a next-generation sequencing library after the exponential amplification stage by introducing the Illumina P5 and P7 primers into the final products, which are then ready for sequencing. Sequencing was performed on the Illumina HiSeq 2500 platform with 2.0 Mb raw reads generated for each sample.

MAIN RESULTS AND THE ROLE OF CHANCE: For PGT-A, BCM and TE biopsy samples showed 90% and 86% clinical concordance with the corresponding BE samples, respectively. In addition, both BCM and TE biopsy samples showed 76% karyotype concordance with the corresponding BE samples. For PGT-SR, we successfully obtained ploidy information for all 23 chromosomes with the exception of any rearrangements involving the Y chromosome. Both BCM and TE biopsy samples showed 100% clinical concordance with the corresponding BE samples in detecting chromosomal rearrangements. BCM and TE biopsy samples showed 90% and 100% karyotype concordance with the corresponding BE samples, respectively. Additionally, no statistically significant differences were detected in the aforementioned values of the BCM and TE biopsy samples in either PGT-A or PGT-SR ($P > 0.05$). Moreover, we achieved accurate quantification of segmental abnormalities using BCM samples. In addition, MICS-Inst reduced the number of steps required for library preparation through the use of new primer designs, resulting in an overall time reduction of 7.5 h. This time reduction allows for the performance of fresh blastocyst transfers.

LIMITATIONS, REASONS FOR CAUTION: The main limitation is that BE, rather the inner cell mass, was used as the standard to evaluate the chromosome screening results.

WIDER IMPLICATIONS OF THE FINDINGS: These results show that MICS-Inst is effective in procedure and precision for PGT, and that it is possible to achieve fresh blastocyst transfer following PGT. The implications are significant, as these findings may lead to minimally invasive PGT methods in the future.

STUDY FUNDING/COMPETING INTEREST(S): This work was supported by the National Natural Science Foundation of China (No. 81671423 and No. 81402130), the National Key Research and Development Program of China (No. 2018YFC1003100), Liaoning Provincial Key Research and Development Program (No. 2018225090), the Fok Ying Tung Education Foundation (No. 151039) and Distinguished Talent Program of Shengjing Hospital (No. ME76). No competing interests declared.

Key words: MICS / chromosomal rearrangement / PGT-SR / PGT-A / culture medium

Introduction

Chromosomal abnormalities, such as balanced translocations, frequently occur in humans (Nielsen and Wohler, 1991). Balanced translocation karyotypes result in quadriradial chromosome formation during meiosis, which then causes a chromosome ploidy imbalance that severely affects normal function and development of the embryo (Alfarawati et al., 2012). To help patients with balanced translocations obtain a healthy live birth, preimplantation genetic testing (PGT) with IVF was developed in the early 1990s to select genetically normal embryos for implantation (Handyside et al., 1990). Fluorescence *in situ* hybridization was first applied in early human embryo biopsies to diagnose balanced translocations (Pehlivan et al., 2003). With the advent of high-throughput genotyping technologies, such as comparative genome hybridization arrays, single nucleotide polymorphism arrays and next-generation sequencing (NGS), PGT has been widely performed to select embryos with balanced chromosomes before implantation (Hu et al., 2016; Lu et al., 2016). With these technologies, PGT has helped tens of thousands of couples worldwide to obtain healthy live births.

A potential risk of the widely used PGT methods for balanced translocation carriers is the use of embryo biopsy before cryopreservation or implantation (Sanchez et al., 2017). IVF embryos can be biopsied at different stages including polar body at Day 1, 8-cell stage embryos or trophoctoderm (TE) cells from blastocyst-stage embryos (BE). Polar body biopsy is noninvasive in principle; however, the procedure is difficult to perform and can only provide information on the maternal genome. Cleavage stage biopsy has been shown to potentially harm development and implantation of the embryo (Scott et al., 2013). Although TE biopsy has been shown to carry less risk to the embryo, it requires a highly trained and skilled embryologist to perform the procedure, which significantly increases the costs of PGT cycles (Xu et al., 2016).

Efforts have been made to achieve noninvasive chromosome detection in embryos. Both blastocoel fluid and spent culture medium contain genetic material (Palini et al., 2013; Tobler et al., 2015; Capalbo et al., 2018) that reflects the chromosome status of the embryo (Gianaroli et al., 2014; Magli et al., 2016). The only barrier to these methods is the low amount of DNA in blastocoel fluid and spent blastocyst medium but this can now be amplified for genetic analysis through whole-genome amplification (WGA) methods and detected through array comparative genomic hybridization and NGS (Shamonki et al., 2016; Xu et al., 2016). Recent studies have shown that blastocoel fluid and spent blastocyst medium could potentially serve as sources for template DNA sampling of the early embryo that can be accessed through noninvasive methods. However, systematic validation of methods that use these noninvasive sources of DNA to

detect balanced translocations are lacking, despite the first live-birth to balanced translocation carriers having been reported in 2016 by our group using a similar method (Xu et al., 2016).

In this report, we present a new assay for minimally invasive chromosome screening (MICS), named MICS-Inst, which achieved high resolution and comprehensive chromosome ploidy detection for all 23 chromosomes using blastocyst culture medium (BCM), TE biopsy and BE samples as template DNA sources. BE was used as the standard to evaluate the chromosome screening results. We validated the assay using 41 vitrified blastocysts donated from 22 couples known to carry a chromosome rearrangement and 21 vitrified blastocysts donated from 8 couples with normal karyotypes and we evaluated the clinical and karyotype concordance with BE by screening for segmental abnormalities.

Materials and Methods

Study design

This study was reviewed and approved by the Reproductive Study Ethics Committee at Shengjing Hospital of China Medical University (research license 2017PS08F). All embryos were obtained from donors at the Center of Reproductive Medicine in Shengjing Hospital of China Medical University. Recruitment took place from May 2018 to August 2018. All donor couples provided informed consent before donating their surplus frozen embryos for research. The donors were financially compensated for the effort, time and inconvenience related to the donation process. A total of 41 blastocysts donated from 22 couples known to carry a chromosome rearrangement and 21 blastocysts donated from 8 couples with normal karyotypes were used in this study. We performed PGT for structural rearrangements (PGT-SR) for 41 BCM, TE biopsy and BE samples as well as PGT for aneuploidies (PGT-A) for 21 BCM, TE biopsy and BE samples. Patient characteristics are provided in Table I and Supplementary Table SI.

BCM, TE and BE sample collection

Good-quality blastocysts, defined as Day 5 and Day 6 embryos \geq BB (AA, AB, BA, BB) based on the Gardner system (Gardner et al., 2000), were used for analysis. A total of 63 samples from couples with normal karyotypes was collected for the application of PGT-A protocols for BCM, TE and BE testing (21 BCM, 21 TE biopsy and 21 BE samples). A total of 123 samples was collected for application of PGT-SR protocols for BCM, TE and BE testing (41 BCM, 41 TE biopsy and 41 BE samples). BCM-thawed blastocysts were placed in 12 μ L droplets of medium for 14 h. Artificial shrinkage of the blastocoel was

Table 1 Unique karyotypes of partners with chromosome rearrangements in couples who donated embryos for PGT-SR.

Karyotype	Number of donors	Number of blastocysts	Balanced chromosomal rearrangements
46,XY,t(1;16)(q21;p12)	1	2	1;16
46,XX,t(2;15)(q33;q14)	1	3	2;15
46,XX,t(3;11)(p25;q22)	1	2	3;11
46,XX,t(3;4)(p25;q21)	1	2	3;4
46,XY,t(4;17)(q28;q25)	1	1	4;17
46,XY,t(4;21)(q12;q11.1)	1	2	4;21
46,XX,t(5;11)(q14;q24)	1	2	5;11
46,XX,t(5;19)(p35;q13)	1	2	5;19
46,XY,t(6;12)(q15;q24)	1	2	6;12
46,XY,t(6;18)(q22.3;q11.2)	1	2	6;18
46,XX,t(7;18)(q21;q12)	1	2	7;18
46,XX,t(8;14)(p23;q21)	1	2	8;14
46,XX,t(9;10)(p13;q11.2)	1	2	9;10
46,XY,t(11;17)(p11.2;p11.2)	1	2	11;17
46,XY,t(12;20)(p12;q11.1)	1	2	12;20
45,XX,rob(13;14)(q10;q10)	5	8	13;14
46,XX,ins(13;22)(q22;q12)	1	2	13;22
46,X,t(X;18)(p22;p11)	1	1	X;18
Total	22	41	

Abbreviation: PGT-SR, PGT for structural rearrangements.

induced by applying a single laser pulse (200 μ s) using ZILOS-tkTM laser system (Hamilton Thorn Bioscience Inc., Beverly, MA, USA) at the junction of TE cells and providing a safe distance from the inner cell mass. After artificial shrinkage, 10 μ L BCM was collected 1 h later and transferred into RNase- and DNase-free PCR tubes containing 5 μ L cell lysis buffer (Yikon Genomics, Shanghai, China). TE biopsy was performed by retrieving 3–5 cells that had herniated through the breach previously opened in the zona pellucida (ZP). When necessary, the biopsy procedure was completed by laser pulses. TE biopsy and BE (no ZP) samples were transferred into RNase- and DNase-free PCR tubes containing 5 μ L cell lysis buffer (Yikon Genomics). All collected samples were frozen immediately in liquid nitrogen and stored at -80°C until further processing.

WGA and library preparation for NGS

BCM, TE biopsy and BE samples were subjected to cell lysis followed by WGA with the multiple annealing and looping-based amplification cycles (MALBAC) technique and library generation. WGA began with a quasilinear Pre-AMP process by annealing a pool of Pre-AMP primers (5'-GCTCTTCCGATCTNNNNNNNN) to the genome template. Pre-AMP primers included a universal sequence in the 5' end and 3–20 random bases in the 3' end that can uniformly hybridize to template DNA. As the temperature was elevated to 72°C , DNA polymerases with strand displacement activity generated semi-amplicons. Amplification of the semi-amplicons generated full amplicons with complementary ends, which allowed the formation of a loop structure during the 63°C cycle, which prevented further amplification and

cross hybridization of the full amplicons. Several improvements and modifications to this method were made in this study. Exponential amplification of the full amplicons was performed by PCR after 5–12 cycles of Pre-AMP with AMP primers 1 and 2 to generate the library for the Illumina NGS platform (Fig. 1; Illumina, San Diego, CA, USA), which combined WGA with library generation and resulted in a reduced preparation time (from 10 to 2.5 h) for NGS.

Sequencing and data analysis

Sequencing was performed on the Illumina HiSeq 2500 platform (Illumina, San Diego, CA, USA) with 2.0 Mb raw reads generated for each sample. Sequencing data were deposited into the NCBI Sequence Read Archive under accession number PRJNA513118 (PGT-SR) and PRJNA524206 (PGT-A). High-quality reads were extracted and mapped to the human hg19 genome. After removing duplicate reads, the read numbers were enumerated along the entire genome and normalized by GC content and a reference dataset. A copy number gain from two to three copies resulted in a 50% increase in read counts, whereas a copy number loss from two copies to one copy resulted in a 50% reduction in read counts. A circular binary segmentation algorithm was used to detect copy number variation (CNV) segments. Using an Illumina HiSeq 2500 platform (Illumina, San Diego, CA, USA), we sequenced the amplified genome of each sample at the depth $\times 0.036$. A total of ~ 110 million bases were sequenced, which is equivalent to 3.6% of the human genome, obtaining an average genome coverage of 3.6%. Such sequencing throughput yields reproducible CNV results with ~ 1 Mb resolution to

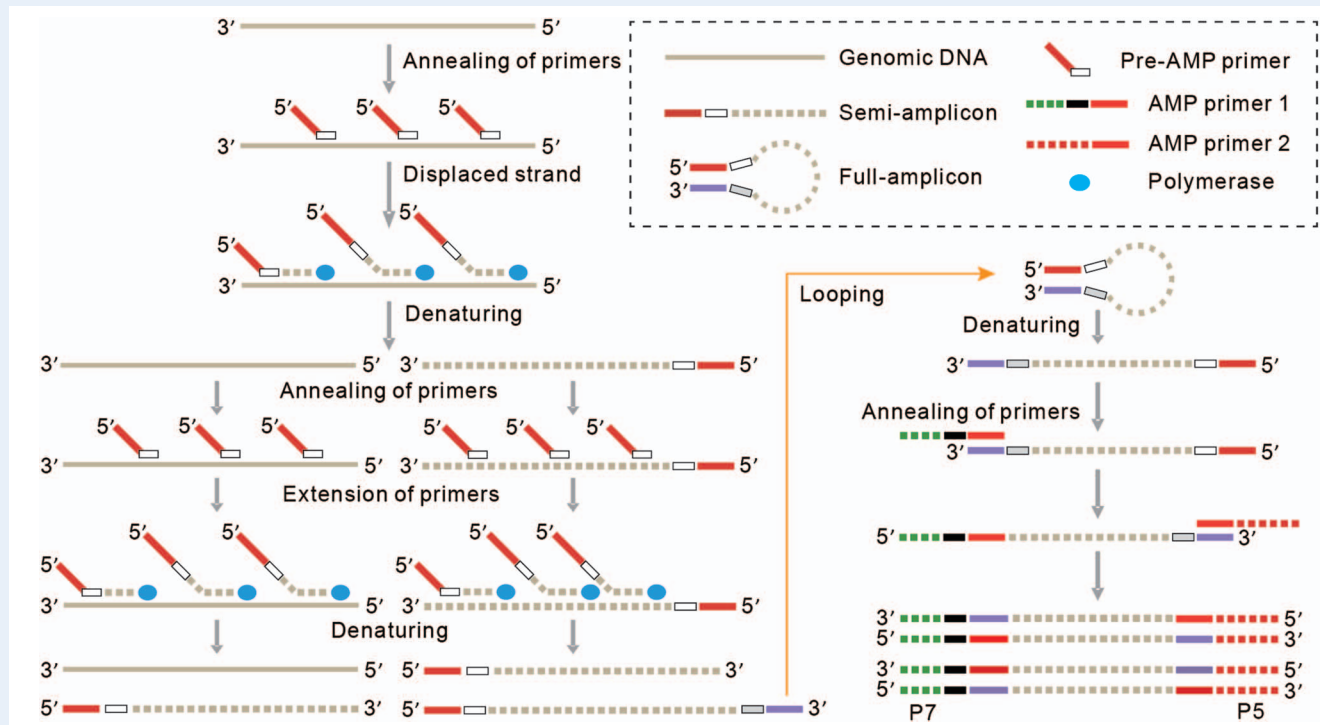


Figure 1 Overview of MICS-Inst. An improved MALBAC whole genome amplification (WGA) strategy was employed. Random primers (preamplification (Pre-AMP) primer) with universal sequences are used to first randomly anneal to genomic DNA molecules and then are extended by DNA polymerase. Universal regions in the Pre-AMP primer enable initial full amplicons to form loops, thereby excluding them as templates for further amplification. After several cycles of linear Pre-AMP, only full amplicons can be exponentially amplified during PCR with AMP primers 1 and 2. The AMP primers have complementary regions that are designed to anneal to the full amplicons. The additional linked sequences of the AMP primers are designed to introduce P7 and P5 primers for the Illumina sequencer platform. By this design, a library ready for sequencing is prepared in one amplification step. The entire process can be accomplished in 2.5 h.

Abbreviations: MICS, minimally invasive chromosome screening; MALBAC, Multiple annealing and looping-based amplification cycles.

detect variations (Hou et al., 2013). Samples were considered normal (euploid) when a copy number $<40\%$ was detected and aneuploid when a copy number $\geq 40\%$ was detected (Cuman et al., 2018). The R program (The R Foundation, Vienna, Austria) was used to graph the copy number of each bin to visualize the CNV profiles of all 23 chromosomes. The high quality rate was calculated as the percentage of raw reads that were high-quality reads. The mapping rate was calculated as the percentage of raw reads that mapped to the human genome. All analyses have been incorporated into a pipeline and can be automatically generated.

Results

A new method for MICS based on MALBAC

We previously reported the WGA method MALBAC, which introduces quasilinear Pre-AMP to reduce the bias associated with nonlinear amplification (Zong et al., 2012) and is suitable for detecting of single nucleotide and CNVs in a single human cell at genome-wide levels. In the present study, we made several significant improvements in MICS-Inst. As demonstrated in Fig. 1, the design of a quasilinear Pre-AMP primer and AMP primers 1 and 2 enables the preparation of an NGS library after the exponential amplification stage by introducing

the Illumina P5 and P7 primers into the final products, which are then ready for sequencing. MICS-Inst shortens the procedure time for WGA and library preparation to 2.5 h as compared to the previously reported >10 h (Zong et al., 2012; Xu et al., 2016). Using the MICS-Inst method, we compared different parameters of sequencing data between BCM, TE biopsy and BE samples. For PGT-A, a total of 21/21 (100%) BCM, TE biopsy and BE samples generated WGA products for NGS (Table II). For PGT-SR, a total of 41/41 (100%) BCM, 39/41 (95.12%) TE biopsy and 41/41 (100%) BE samples generated WGA products for NGS (Table III). All three sample types generated a high rate of high-quality reads and mapping reads, which indicates that the approach has good uniformity. Moreover, no significant differences in these parameters were detected between the BCM and TE biopsy samples (Supplementary Table SII).

Comparison of BCM results using MICS-Inst with TE and BE

To validate the reliability of MICS-Inst, we first performed PGT-A on 21 BCM and TE biopsy samples and compared them to corresponding BE samples. As shown in Tables II and IV, BCM and TE biopsy samples showed 90.48% and 85.71% clinical concordance with the corresponding BE samples, respectively. In addition, both BCM and TE biopsy

Table II PGT-A; results from BCM, TE and BE samples.

No.	BCM	BE	TE
NK1	-3,+13,-21,XX	-3,+13,-21,XX	-2,-3,+13,-21,XX
NK2	46,XX	46,XX	46,XX
NK3	+1,+9,XY	46,XY	+1,+14,+15,+18,XY
NK4	46,XX	46,XX	46,XX
NK5	-15q(q14 → q25.3,~53 M),XY	46,XY	-15q(q26.1 → qter,~11 M),XY
NK6	46,XY	46,XY	46,XY
NK7	46,XX	46,XX	46,XX
NK8	-5,XX	-18,XX	-5q,XX
NK9	-16,XY	-16,XY	-16,XY
NK10	46,XX	46,XX	46,XX
NK11	46,XX	46,XX	46,XX
NK12	46,XX	46,XX	-Xq(q13.3 → qter,~80 M),XX
NK13	+22,XY	+22,XY	+22,XY
NK14	46,XY	46,XY	46,XY
NK15	-8q(q21.13 → qter,~61 M), -9q(q21.11 → qter,~69 M), -12,XX	-8q(q21.13 → qter,~61 M),XX	-8q(q21.13 → qter,~61 M),XX
NK16	46,XY	46,XY	46,XY
NK17	-9,XX	-9p,XX	-9p,XX
NK18	46,XX	46,XX	46,XX
NK19	46,XY	46,XY	46,XY
NK20	46,XY	46,XY	46,XY
NK21	46,XY	46,XY	46,XY

Abbreviations: NK, normal karyotype; BCM, blastocyst culture medium; TE, trophectoderm; BE, blastocyst-stage embryo.

samples showed 76.19% karyotype concordance with the corresponding BE samples. To further validate the accuracy of MICS-Inst, we performed PGT-SR on 41 BCM and TE biopsy samples and compared them to the corresponding BE samples. The donor karyotypes are summarized in Table I. As a general overview of concordance in chromosomal rearrangements detected in each sample, the read count distribution across all 23 chromosomes for a sample of 15 blastocysts is provided in Fig. 2, results for the remaining 26 blastocysts are shown in Supplementary Fig. S1. For PGT-SR, we successfully obtained ploidy information for all 23 chromosomes, with the exception of rearrangements involving the Y chromosome, from 41 BCM and TE biopsy samples and compared them to the corresponding BE samples. As shown in Tables III and IV, BCM and TE biopsy samples showed 100% clinical concordance with the corresponding BE samples in detecting chromosomal rearrangements. BCM and TE biopsy samples showed 90.24% and 100% karyotype concordance with the corresponding BE samples, respectively. Notably, no significant differences in the aforementioned values were detected between BCM and TE biopsy samples ($P > 0.05$).

Discussion

Previous studies have demonstrated that BCM is a viable source of genomic DNA for use in PGT (Xu *et al.*, 2016). However, the value

of this BCM method in screening for embryonic chromosomal rearrangements has not been systematically compared with that of BE and TE biopsy in the same blastocyst. In this study, we first systematically performed PGT-SR on BCM, TE and BE samples using blastocoel fluid mixed with spent blastocyst medium and made several significant improvements to the pre-existing MALBAC WGA techniques, thereby reducing the number of steps required for library preparation through the use of new primer designs, which resulted in an overall time reduction of 7.5 h. With this time reduction, the MICS-Inst procedure could be implemented in a PGT treatment cycle under clinical conditions, and embryos undergoing this method can undergo a fresh blastocyst transfer following PGT.

Until recently, the clinical use of BCM for PGT was a controversial issue (Shamonki *et al.*, 2016; Xu *et al.*, 2016; Capalbo *et al.*, 2018); however, several improvements to the technique have been made, such as DNA collection, amplification and sequencing methods, that increase the amount of free embryonic DNA and prevent non-embryonic DNA interference. It is well known that the total amount of DNA in BCM is the limitation for CNV detection. Capalbo *et al.* (2018) compared the diagnostic efficacy of blastocoel fluid and spent blastocyst medium as sources of DNA for PGT. The results showed that only eight blastocoel fluid samples (34.8%) could be amplified in PGT-A. Regarding PGT for monogenic disease, successful amplification occurred in 27.4% and 89.7% of blastocoel fluid and spent blastocyst medium samples, respectively (Capalbo *et al.*, 2018). These

Table III PGT-SR; results from BCM, TE and BE samples by chromosome rearrangement in couples.

	BCM	BE	TE
46,XY,t(6;18)(q22.3;q11.2)			
CR1	−6q(q22.31 → qter,~50 M,×1) +18q(q11.2 → qter,~56 M,×3)	−6q(q22.31 → qter,~50 M,×1) +18q(q11.2 → qter,~56 M,×3)	−6q(q22.31 → qter,~50 M,×1) +18q(q11.2 → qter,~56 M,×3)
CR2	−6q(q22.31 → qter,~50 M,×1) +18q(q11.2 → qter,~56 M,×3)	−6q(q22.31 → qter,~50 M,×1) +18q(q11.2 → qter,~56 M,×3)	−6q(q22.31 → qter,~50 M,×1) +18q(q11.2 → qter,~56 M,×3)
46,XY,t(6;12)(q15;q24)			
CR3	+6p(×3) +6q(q11.1 → q15,~28 M,×3) −12(×1)	+6p(×3) +6q(q11.1 → q15,~28 M,×3) −12(×1)	N/A N/A
CR4	−6q(q15 → qter,~76 M,×1) +12q(qter → qter,~4.1 M,×3)	−6q(q15 → qter,~76 M,×1) +12q(qter → qter,~4.1 M,×3)	−6q(q15 → qter,~76 M,×1) +12q(qter → qter,~4.1 M,×3)
46,XY,t(4;21)(q12;q11.1)			
CR5	−4p(×1)	−4p(×1)	−4p(×1)
CR6	+4p(×3) −21(×1)	+4p(×3) −	+4p(×3) −
46,XY,t(4;17)(q28;q25)			
CR7	−4q(q28.1 → q34.1,~51 M,×1)	+4p(p16.1 → p15.2,~17 M,×3), −4q(q28.1 → q33,~48 M,×1), −4q(q34.1 → qter,~19 M,×1)	+4p(p16.1 → p15.2,~17 M,×3) −4q(q28.1 → q33,~48 M,×1), −4q(q34.1 → qter,~19 M,×1),
46,XY,t(12;20)(p12;q11.1)			
CR8	+20q(×3) −12p(×1)	+20q(×3) −12p(×1)	+20q(×3) −12p(×1)
CR9	+12q(×3) −20p(×1)	+12q(×3) −20p(×1)	+12q(×3) −20p(×1)
46,XY,t(11;17)(p11.2;p11.2)			
CR10	+11p(×3) −17p(pter → p12,~11 M,×1)	+11p(×3) −17p(pter → p12,~11 M,×1)	N/A N/A
CR11	+11p(×3) −17p(pter → p12,~11 M,×1)	+11p(×3) −17p(pter → p12,~11 M,×1)	+11p(×3) −17p(pter → p12,~11 M,×1)
46,XY,t(1;16)(q21;p12)			
CR12	−1q(×1) +16q(×3)	−1q(×1) +16q(×3)	−1q(×1) +16q(×3)
CR13	+1p(×3) −16p(×1)	+1p(×3) −16p(×1)	+1p(×3) −16p(×1)
46,XX,t(9;10)(p13;q11.2)			
CR14	+9p(×3) −10p(×1)	+9p(×3) −10p(×1)	+9p(×3) −10p(×1)
CR15	−9p(×1) +10p(×3)	−9p(×1) +10p(×3)	−9p(×1) +10p(×3)
46,XX,t(8;14)(p23;q21)			
CR16	−8p(pter → p23.1,~12 M,×1) +14q(q21.1 → qter,~67 M,×3)	−8p(pter → p23.1,~12 M,×1) +14q(q21.1 → qter,~67 M,×3)	−8p(pter → p23.1,~12 M,×1) +14q(q21.1 → qter,~67 M,×3)
CR17	+8p(pter → p23.1,~12 M,×3) +14q(q11.2 → q21.1,~19 M,×3)	+8p(pter → p23.1,~12 M,×3) +14q(q11.2 → q21.1,~19 M,×3)	+8p(pter → p23.1,~12 M,×3) +14q(q11.2 → q21.1,~19 M,×3)

(Continued)

Table III Continued

	BCM	BE	TE
46,XX,t(7;18)(q21;q12)			
CR18	–7q(q21.13 → qter,~69 M, × 1), +18q(q12.2 → q23,~41 M, × 3)	–7q(q21.13 → qter,~69 M, × 1) +18q(q12.2 → q23,~41 M, × 3)	–7q(q21.13 → qter,~69 M, × 1) +18q(q12.2 → q23,~41 M, × 3)
CR19	–7q(q21.13 → qter,~69 M, × 1) –18p(× 1)	–7q(q21.13 → qter,~69 M, × 1) –18p(× 1)	–7q(q21.13 → qter,~69 M, × 1) –18p(× 1)
46,XX,t(5;19)(p35;q13)			
CR20	–19p(× 1), –19q(q13.11 → q13.31,~10.4 M, × 1) –5q(qter → qter,~1.5 M, × 1)	+19q(q13.32 → qter,~13 M, × 3) –5q(qter → qter,~1.5 M, × 1)	+19q(q13.32 → qter,~13 M, × 3) –5q(qter → qter,~1.5 M, × 1)
CR21	+19q(q13.32 → qter,~13 M, × 3) –5q(qter → qter,~1.5 M, × 1)	+19q(q13.32 → qter,~13 M, × 3) –5q(qter → qter,~1.5 M, × 1)	+19q(q13.32 → qter,~13 M, × 3) –5q(qter → qter,~1.5 M, × 1)
46,XX,t(5;11)(q14;q24)			
CR22	–5q(q14.1 → qter,~100 M, × 1) +11q(q24.1 → qter,~11 M, × 3)	–5q(q14.1 → qter,~100 M, × 1) +11q(q24.1 → qter,~11 M, × 3)	–5q(q14.1 → qter,~100 M, × 1) +11q(q24.1 → qter,~11 M, × 3)
CR23	–5q(q14.1 → qter,~100 M, × 1) +11q(q24.1 → qter,~11 M, × 3)	–5q(q14.1 → qter,~100 M, × 1) +11q(q24.1 → qter,~11 M, × 3)	–5q(q14.1 → qter,~100 M, × 1) +11q(q24.1 → qter,~11 M, × 3)
46,XX,t(3;4)(p25;q21)			
CR24	–3p(pter → p25.3,~10 M, × 1) +4q(× 3)	–3p(pter → p25.3,~10 M, × 1) +4q(× 3)	–3p(pter → p25.3,~10 M, × 1) +4q(× 3)
CR25	–3p(pter → p25.3,~10 M, × 1), +4q(× 3)	–3p(pter → p25.3,~10 M, × 1) +4q(× 3)	–3p(pter → p25.3,~10 M, × 1) +4q(× 3)
46,XX,t(3;11)(p25;q22)			
CR26	–11q(q22.1 → qter,~33 M, × 1) –	–11q(q22.1 → qter,~33 M, × 1) +3p(pter → pter,~1.8 M, × 3)	–11q(q22.1 → qter,~33 M, × 1) +3p(pter → pter,~1.8 M, × 3)
CR27	–11q(q22.1 → qter,~33 M, × 1) –	–11q(q22.1 → qter,~33 M, × 1) +3p(pter → pter,~1.8 M, × 3)	–11q(q22.1 → qter,~33 M, × 1) +3p(pter → pter,~1.8 M, × 3)
46,XX,t(2;15)(q33;q14)			
CR28	+2p(× 3), +2q(q11.1 → q33.2,~109 M, × 3), –2q(q33.3 → q37.3,~34 M, × 1) –15q(q11.2 → q14,~11 M, × 1), +15q(q14 → q26.3,~67 M, × 3)	+2p(× 3), +2q(q11.1 → q33.2,~109 M, × 3), –2q(q33.3 → q37.3,~34 M, × 1) –15q(q11.2 → q14,~11 M, × 1), +15q(q14 → q26.3,~67 M, × 3)	+2p(× 3), +2q(q11.1 → q33.2,~109 M, × 3), –2q(q33.3 → q37.3,~34 M, × 1) –15q(q11.2 → q14,~11 M, × 1), +15q(q14 → q26.3,~67 M, × 3)
CR29	+2q(q33.3 → q37.3,~34 M, × 3) –15q(q14 → q26.3,~67 M, × 1)	+2q(q33.3 → q37.3,~34 M, × 3) –15q(q14 → q26.3,~67 M, × 1)	+2q(q33.3 → q37.3,~34 M, × 3) –15q(q14 → q26.3,~67 M, × 1)
CR30	–2q(q33.3 → q37.3,~34 M, × 1) +15q(q14 → q26.3,~67 M, × 3)	–2q(q33.3 → q37.3,~34 M, × 1) +15q(q14 → q26.3,~67 M, × 3)	–2q(q33.3 → q37.3,~34 M, × 1) +15q(q14 → q26.3,~67 M, × 3)
46,X,t(X;18)(p22;p11)			
CR31	–X(× 1) +18q(× 3)	–X(× 1) +18q(× 3)	–X(× 1) +18q(× 3)
46,XX,ins(13;22)(q22;q12)			
CR32	–22q(q12.2 → q13.31,~18 M, × 1)	–22q(q12.2 → q13.31,~18 M, × 1)	–22q(q12.2 → q13.31,~18 M, × 1)
CR33	+22q(q12.2 → q13.31,~18 M, × 3)	+22q(q12.2 → q13.31,~18 M, × 3)	+22q(q12.2 → q13.31,~18 M, × 3)
45,XX,rob(13;14)(q10;q10)			
CR34	–14(× 1)	–14(× 1)	–14(× 1)
CR35	+13(× 3)	+13(× 3)	+13(× 3)
CR36	+14(× 3)	+14(× 3)	+14(× 3)
CR37	+14(× 3)	+14(× 3)	+14(× 3)

(Continued)

Table III Continued

	BCM	BE	TE
CR38	—	—	—
CR39	+14(×3)	+14(×3)	+14(×3)
CR40	+14(×3)	+14(×3)	+14(×3)
CR41	+13(×3)	+13(×3)	+13(×3)
	—14(×1)	—14(×1)	—14(×1)

Abbreviations: CR, chromosomal rearrangement; —, no balanced CRs were detected; N/A, not applicable.

Table IV Clinical and karyotype concordance of PGT. Shown PGT-A and PGT-SR between BCM, TE and BE samples.

PGT-A	BCM and BE	TE and BE	p value
Clinical concordance	19/21 (90.48%)	18/21 (85.71%)	0.9847
Karyotype concordance	16/21 (76.19%)	16/21 (76.19%)	0.7171
PGT-SR			
Clinical concordance	41/41 (100%)	39/39 (100%)	N/A
Karyotype concordance	37/41 (90.24%)	39/39 (100%)	0.1366

Abbreviations: N/A, not applicable.

observations raise the possibility that the detection rate may be improved by mixing blastocoel fluid and spent blastocyst medium samples, which is denoted as BCM in this study. To achieve this, thawed blastocysts were placed in 12 μ L droplets of medium for 14 h. After artificial shrinkage, the blastocysts were consecutively placed in the same droplets for 1 h for blastocoel fluid release. Unexpectedly, the PGT-SR amplification rates for BCM reached 100%. To date and to the best of our knowledge, only Kuznyetsov et al. (2018) and Li et al. (2018) performed PGT-A using the same culture medium collection method. Kuznyetsov et al. (2018) confirmed that the combination of blastocoel fluid and spent blastocyst medium contains sufficient embryonic DNA for WGA using the SurePlex WGA method and were able to achieve accurate aneuploidy screening. Li et al. (2018) used discarded embryos, which are not suitable for transfer and may be the primary reason for the relatively high discordance among the BCM, TE and BE samples. Predictably, the higher DNA amplification rates were due to increased DNA availability caused by mixing blastocoel fluid and spent blastocyst medium samples. As mentioned earlier, NGS cannot be efficiently performed when the DNA concentration after amplification is below 10 ng/ml (Li et al., 2018). The DNA library concentration for this method was 38.88 ± 24.08 ng/ml for BCM (Supplementary Table SII). At this DNA library concentration, we completed the karyotype assessment and achieved accurate quantification of segmental abnormalities using BCM samples.

The current understanding of the source of cell-free DNA in blastocyst culture media is limited. One possibility is that DNA in the culture media may derive from cells damaged due to the laser pulses used during artificial shrinkage, although in the present study, the laser pulse was used at the junction of TE cells and provided a safe distance from the inner cell mass. In addition, as previously shown,

cell-free DNA may derive from cells discarded by the embryos as a self-correction mechanism against aneuploidies (Hammond et al., 2017). However, this view was challenged recently due to the discovery that the amount of cell-free DNA was not significantly greater in culture media from aneuploid embryos as compared to euploid embryos (Vera-Rodriguez et al., 2018). Vera-Rodriguez et al. (2018) suggested that cell-free DNA from culture medium represents a mix of maternal and embryonic DNA. Notably, it has been observed that levels of nuclear DNA and mitochondrial DNA were increased in culture medium at the blastocyst stage (Hammond et al., 2017), and the accuracy of the PGT using culture medium was markedly improved by delaying the start of incubation until Day 4 (Lane et al., 2017). This could be explained by the gradual decrease of the influence of maternal DNA on cell-free DNA of culture medium as the embryonic DNA concentration increases at later stages because the number of embryonic cells increases exponentially during development. It is known that contamination by maternal DNA often leads to female bias in the sex ratio. As shown in our study, all sex chromosomes were consistent among the BCM, TE biopsy and BE samples, and the sex ratio was balanced (XX:XY = 11:10; Table II). These results provide indirect evidence that is suggestive of no contamination by maternal DNA. In addition, although theoretically cumulus cells can be effectively removed during the denudation process prior to ICSI in fresh cycle, the effect is limited in its capacity to avoid the contamination of maternal DNA in clinical settings (Hammond et al., 2017; Vera-Rodriguez et al., 2018). However, as shown in our study, by using BCM derived from cryopreserved blastocysts, we observed higher clinical and karyotype concordance (Table IV). This reminds us that the freeze-thaw process and reagent concentration variation are very effective in eliminating cumulus cells and reducing the impact of maternal DNA. Another interesting point is whether the freeze-thaw process may

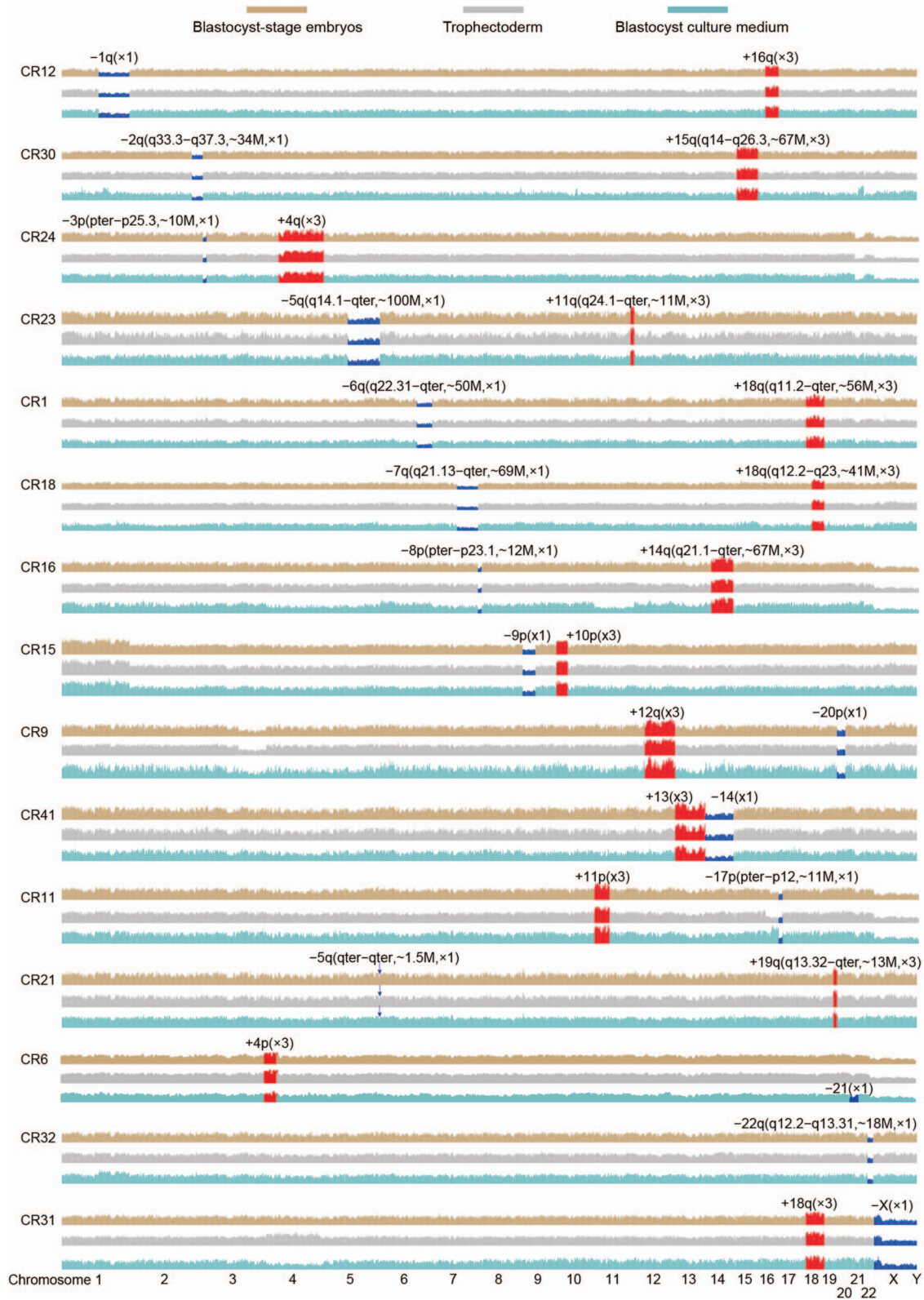


Figure 2 Demonstration of read count distribution on chromosomes in PGT-SR-derived blastocyst samples. Read numbers were counted in each bin and are shown across 22 autosomes and the X chromosome. BE, TE biopsy and BCM patterns from the same blastocyst were compared. Copy number gains and losses related to translocation chromosomes are presented in red and in blue, respectively. A total of 15/41 blastocysts were selected to cover variations across all 23 chromosomes, remaining chromosomes (26/41) are shown in [Supplementary Figure S1](#).

influence the release of cell-free DNA. Currently, this subject is poorly understood and is therefore a question that is worthy of further investigation.

Our results show that both BCM collection and MICS-Inst methods are effective in procedure and precision for PGT. We also demonstrated that it is possible to achieve fresh blastocyst transfer after PGT using MICS-Inst methods. The implications are significant, as these findings may allow for a minimally invasive method for PGT in the future.

Supplementary data

Supplementary data are available at *Human Reproduction* online.

Authors' roles

X.X.W., D.L., S.J.L and J.J. conceived and designed the study. J.J., D.L., B.S., M.S., D.L.Y., Y.X.Y., W.L.L. and L.S. performed data acquisition and interpretation. X.X.W., D.L., S.J.L and M.S. wrote the paper. All authors approved the final manuscript.

Funding

National Natural Science Foundation of China (No. 81671423 and No. 81402130); the National Key Research and Development Program of China (No. 2018YFC1003100); Liaoning Provincial Key Research and Development Program (No. 2018225090); the Fok Ying Tung Education Foundation (No. 151039); Distinguished Talent Program of Shengjing Hospital (No. ME76).

Conflict of interest

No competing interests declared.

References

- Alfarawati S, Fragouli E, Colls P, Wells D. Embryos of robertsonian translocation carriers exhibit a mitotic interchromosomal effect that enhances genetic instability during early development. *PLoS Genet* 2012;**8**:e1003025.
- Capalbo A, Romanelli V, Patassini C, Poli M, Girardi L, Giancani A, Stoppa M, Cimadomo D, Ubaldi FM, Rienzi L. Diagnostic efficacy of blastocoel fluid and spent media as sources of DNA for preimplantation genetic testing in standard clinical conditions. *Fertil Steril* 2018;**110**:870–879.
- Cuman C, Beyer CE, Brodie D, Fullston T, Lin JI, Willats E, Zander-Fox D, Mullen J. Defining the limits of detection for chromosome rearrangements in the preimplantation embryo using next generation sequencing. *Hum Reprod* 2018;10.1093/humrep/dey227.
- Gardner DK, Lane M, Stevens J, Schlenker T, Schoolcraft WB. Blastocyst score affects implantation and pregnancy outcome: towards a single blastocyst transfer. *Fertil Steril* 2000;**73**:1155–1158.
- Gianaroli L, Magli MC, Pomante A, Crivello AM, Cafueri G, Valerio M, Ferraretti AP. Blastocentesis: a source of DNA for preimplantation genetic testing. Results from a pilot study. *Fertil Steril* 2014;**102**:1692–1699.
- Hammond ER, McGillivray BC, Wicker SM, Peek JC, Shelling AN, Stone P, Chamley LW, Cree LM. Characterizing nuclear and mitochondrial DNA in spent embryo culture media: genetic contamination identified. *Fertil Steril* 2017;**107**:220–228.
- Handyside AH, Kontogianni EH, Hardy K, Winston RM. Pregnancies from biopsied human preimplantation embryos sexed by Y-specific DNA amplification. *Nature* 1990;**344**:768–770.
- Hou Y, Fan W, Yan L, Li R, Lian Y, Huang J, Li J, Xu L, Tang F, Xie XS et al. Genome analyses of single human oocytes. *Cell* 2013;**155**:1492–1506.
- Hu L, Cheng D, Gong F, Lu C, Tan Y, Luo K, Wu X, He W, Xie P, Feng T et al. Reciprocal translocation carrier diagnosis in preimplantation human embryos. *EBioMedicine* 2016;**14**:139–147.
- Kuznetsov V, Madjunkova S, Antes R, Abramov R, Motamedi G, Ibarrientos Z, Librach C. Evaluation of a novel non-invasive preimplantation genetic screening approach. *PLoS One* 2018;**13**:e0197262.
- Lane M, Zander-Fox D, Hamilton H, Jasper MJ, Hodgson BL, Fraser M, Bell F. Ability to detect aneuploidy from cell free DNA collected from media is dependent on the stage of development of the embryo. *Fertil Steril* 2017;**108**:e61.
- Li P, Song Z, Yao Y, Huang T, Mao R, Huang J, Ma Y, Dong X, Huang W, Huang J et al. Preimplantation genetic screening with spent culture medium/blastocoel fluid for in vitro fertilization. *Sci Rep* 2018;**8**:9275.
- Lu L, Lv B, Huang K, Xue Z, Zhu X, Fan G. Recent advances in preimplantation genetic diagnosis and screening. *J Assist Reprod Genet* 2016;**33**:1129–1134.
- Magli MC, Pomante A, Cafueri G, Valerio M, Crippa A, Ferraretti AP, Gianaroli L. Preimplantation genetic testing: polar bodies, blastomeres, trophectoderm cells, or blastocoelic fluid? *Fertil Steril* 2016;**105**:676–683.
- Nielsen J, Wohler M. Chromosome abnormalities found among 34,910 newborn children: results from a 13-year incidence study in Arhus, Denmark. *Hum Genet* 1991;**87**:81–83.
- Palini S, Galluzzi L, De Stefani S, Bianchi M, Wells D, Magnani M, Bulletti C. Genomic DNA in human blastocoele fluid. *Reprod Biomed Online* 2013;**26**:603–610.
- Pehlivan T, Rubio C, Rodrigo L, Remohi J, Pellicer A, Simon C. Preimplantation genetic diagnosis by fluorescence in situ hybridization: clinical possibilities and pitfalls. *J Soc Gynecol Investig* 2003;**10**:315–322.
- Sanchez T, Seidler EA, Gardner DK, Needleman D, Sakkas D. Will noninvasive methods surpass invasive for assessing gametes and embryos? *Fertil Steril* 2017;**108**:730–737.
- Scott RT Jr, Upham KM, Forman EJ, Zhao T, Treff NR. Cleavage-stage biopsy significantly impairs human embryonic implantation potential while blastocyst biopsy does not: a randomized and paired clinical trial. *Fertil Steril* 2013;**100**:624–630.
- Shamoni MI, Jin H, Haimowitz Z, Liu L. Proof of concept: preimplantation genetic screening without embryo biopsy through analysis of cell-free DNA in spent embryo culture media. *Fertil Steril* 2016;**106**:1312–1318.

- Tobler KJ, Zhao Y, Ross R, Benner AT, Xu X, Du L, Broman K, Thrift K, Brezina PR, Kearns WG. Blastocoel fluid from differentiated blastocysts harbors embryonic genomic material capable of a whole-genome deoxyribonucleic acid amplification and comprehensive chromosome microarray analysis. *Fertil Steril* 2015; **104**:418–425.
- Vera-Rodriguez M, Diez-Juan A, Jimenez-Almazan J, Martinez S, Navarro R, Peinado V, Mercader A, Meseguer M, Blesa D, Moreno I et al. Origin and composition of cell-free DNA in spent medium from human embryo culture during preimplantation development. *Hum Reprod* 2018; **33**:745–756.
- Xu J, Fang R, Chen L, Chen D, Xiao JP, Yang W, Wang H, Song X, Ma T, Bo S et al. Noninvasive chromosome screening of human embryos by genome sequencing of embryo culture medium for in vitro fertilization. *Proc Natl Acad Sci U S A* 2016; **113**:11907–11912.
- Zong C, Lu S, Chapman AR, Xie XS. Genome-wide detection of single-nucleotide and copy-number variations of a single human cell. *Science* 2012; **338**:1622–1626.